ISSN 0021-3640, JETP Letters, 2014, Vol. 99, No. 10, pp. 565–569. © Pleiades Publishing, Inc., 2014.
Original Russian Text © I.A. Tarasov, Z.I. Popov, S.N. Varnakov, M.S. Molokeev, A.S. Fedorov, I.A. Yakovlev, D.A. Fedorov, S.G. Ovchinnikov, 2014, published in Pis'ma v Zhurnal Eksperimental'noi i Teoreticheskoi Fiziki, 2014, Vol. 99, No. 10, pp. 651–655.

Optical Characteristics of an Epitaxial Fe_3Si/Si(111) Iron Silicide Film

I. A. Tarasov[a, b, *], Z. I. Popov[a, b], S. N. Varnakov[a, b], M. S. Molokeev[a], A. S. Fedorov[a], I. A. Yakovlev[a], D. A. Fedorov[a], and S. G. Ovchinnikov[a, b]

[a] *Kirensky Institute of Physics, Siberian Branch, Russian Academy of Sciences, Akademgorodok, Krasnoyarsk, 660036 Russia*

[b] *Siberian State Aerospace University, Krasnoyarsk, 660014 Russia*

* *e-mail: tia@iph.krasn.ru*

Received April 18, 2014

The dispersion of the relative permittivity ε of a 27-nm-thick epitaxial Fe_3Si iron silicide film has been measured within the $E = 1.16–4.96$ eV energy range using the spectroscopic ellipsometry technique. The experimental data are compared to the relative permittivity calculated in the framework of the density functional theory using the GGA–PBE approximation. For Fe_3Si, the electronic structure and the electronic density of states (DOS) are calculated. The analysis of the frequencies corresponding to the transitions between the DOS peaks demonstrates qualitative agreement with the measured absorption peaks. The analysis of the single wavelength laser ellipsometry data obtained in the course of the film growth demonstrates that a continuous layer of Fe_3Si iron silicide film is formed if the film thickness achieves 5 nm.

DOI: 10.1134/S0021364014100105

1. Currently, ferromagnetic iron silicide Fe_3Si turns out to be a promising material for such applications as spin transistors, magnetoresistive memory, and magneto-optical devices [1–4] owing to its high Curie temperature (about 840 K), relatively high magnetic permeability, low magnetic and crystallographic anisotropy, high electrical resistivity, and high spin polarization (as high as 43%). During the last decade, thin films of this material have been widely studied. A lot of papers deal with the interplay of their structural and magnetic characteristics [5, 6], as well as with the transport properties and developments of prototypes of spintronic devices [7, 8]. However, the electronic structure and optical properties of Fe_3Si are still rather poorly studied. In particular, the energy dependence of its relative permittivity is treated only in one theoretical paper [9], the results of which have not been verified by experiment. The main aims of our work are to study the optical characteristics of an epitaxial Fe_3Si/Si(111) iron silicide film and to determine the dispersion of the relative permittivity ε using the spectroscopic ellipsometry technique.

2. The Fe_3Si film was obtained by the thermal evaporation technique in ultrahigh vacuum at the reconstructed Si(111)7 × 7 surface. The formation of the film structure was controlled by an LEF-751M high-speed laser ellipsometer [10]. The technique used for the preparation of the atomically clean Si(111)7 × 7 surface, the process of growth of Fe_3Si/Si(111)7 × 7 film, and the data on the structure of this film and its magnetic properties were described in [11].

The data obtained by single wavelength ellipsometry for the synthesized Fe_3Si/Si(111) film (Fig. 1) were analyzed by the method described in [12]. This analysis was based on the optical model involving a homogeneous isotropic film at a semi-infinite isotropic substrate. The value obtained for the thickness of the formed film agrees well with the data provided by transmission electron microscopy. It equals 27 nm.

In Fig. 1, we can see that the behavior of the thickness at the initial stages of the film growth is not physical. The calculated refractive index n and the coefficient of absorption k vary drastically beginning from values close to the optical parameters of silicon ($n = 3.93$ and $k = 0.54$) to those characteristic of conducting materials ($n = 3.43$ and $k = 3.54$). We attribute such behavior at the initial stage of the film formation to the epitaxial island growth mechanism, rather than to layer-by-layer growth. After 45 min of film growth, the thickness begins growing monotonically and n and k achieve values remaining unchanged in the course of further growth. Thus, when the effective thickness achieves 5 nm, the Fe_3Si film forms as a continuous layer. The values of the real and imaginary parts of the relative permittivity determined by the laser ellipsometry ($\lambda = 632.8$ nm) at a temperature of 150° are $\varepsilon' = -0.97$ and $\varepsilon'' = 24.07$, respectively.

3. In the present work, the energy dependence of the relative permittivity is calculated from the data of multiangle spectroscopic ellipsometry using the method described in detail in [13]. In the calculations, we used the optical model involving a homogeneous

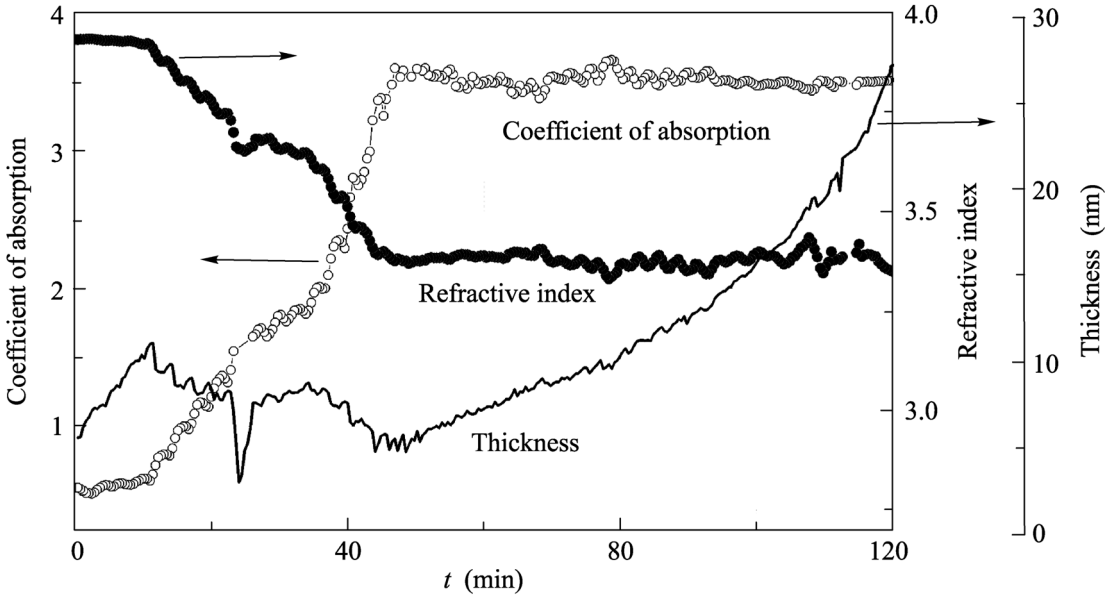

Fig. 1. Refractive index, coefficient of absorption, and thickness of $Fe_3Si/Si(111)$ film versus time of deposition.

isotropic film with unknown thickness and relative permittivity on an isotropic Si substrate with known optical characteristics. The measurements were performed at $T = 296$ K using an Ellips-1801 high-speed spectral ellipsometer.

The computational algorithms used were tested through the use of a thin polycrystalline film of semiconducting β-$FeSi_2$ iron disilicide on a Si(100) substrate with well-studied optical characteristics [14]. The semiconducting disilicide film was also produced by the thermal evaporation technique in ultrahigh vacuum on the reconstructed Si(100)2 × 1 surface. The substrate surface temperature was 450°C. The X-ray structural analysis performed using a D8 ADVANCE powder diffractometer (Cu $K\alpha_{1,2}$ radiation, Ni filter) with a VANTEC linear detector demonstrates that the polycrystalline iron disilicide film forms with the preferable orientation corresponding to the (331) crystallographic plane (see Fig. 2a). The calculated energy dependence of the real (ε') and imaginary (ε") parts of the relative permittivity is shown in Fig. 2b. The results of the calculations agree well with the experimental data for the polycrystalline thin-film and bulk β-$FeSi_2$ samples reported in [14].

4. It is well known that Fe_3Si silicide crystallizes according to three crystallographic types: A_2, B_2, and DO_3. The DO_3 type is an ordered phase and has atomic packing [4] similar to that of Heusler alloys of $L2_1$ type. The electronic and geometric structures of DO_3 type Fe_3Si silicide were calculated by quantum chemistry simulations based on the licensed program package VASP 5.3 [15–17] in the framework of the density functional theory (DFT) using the plane wave basis and the projector augmented wave (PAW) formalism [18, 19]. To describe the exchange-correlation functional, we use the generalized gradient approximation (GGA) involving also the Perdew–Burke–Ernzerhof (PBE) approximation [20]. For optimization of the unit cell geometry of Fe_3Si (*Fm*-3*m*), the first Brillouin zone in the reciprocal space is automatically divided into a 6 × 6 × 6 mesh chosen according to the Monkhorst–Pack scheme [21]. In the calculations, the cutoff energy E_{cutoff} is equal to 293 eV. In the modeling of the structure under study, the optimization of the geometry is performed up to maximum values of the forces acting on atoms and equal to 0.01 eV/A. After calculation of the ground state by the VASP program, we calculate the frequency-dependent dielectric matrix. The details of this method are described in [22].

In Figs. 3a and 3b, we show the real (ε') and imaginary (ε") parts of the measured energy-dependent relative permittivity of the epitaxial Fe_3Si film for the energies E of the incident light wave ranging from 1.16 to 4.96 eV, which are determined according the aforementioned methods [13]. In these figures, we also illustrate the results of the ab initio calculations of the energy dependence of ε' and ε".

In Figs. 3a and 3b, we can see that the measured and calculated real and imaginary parts of the relative permittivity are in good qualitative agreement with each other. At the same time, the calculated curves exhibit several clearly pronounced peaks. In particular, for ε", the peaks are centered within the $E_1^t - E_5^t$ range at energies equal to 1.7, 2.66, 3.62, 4.49, and 5.12 eV. After fitting the measured curves by Gaussian functions (see Fig. 3b), we can distinguish only four peaks corresponding to 1.2, 3.16, 4, and 4.86 eV. The

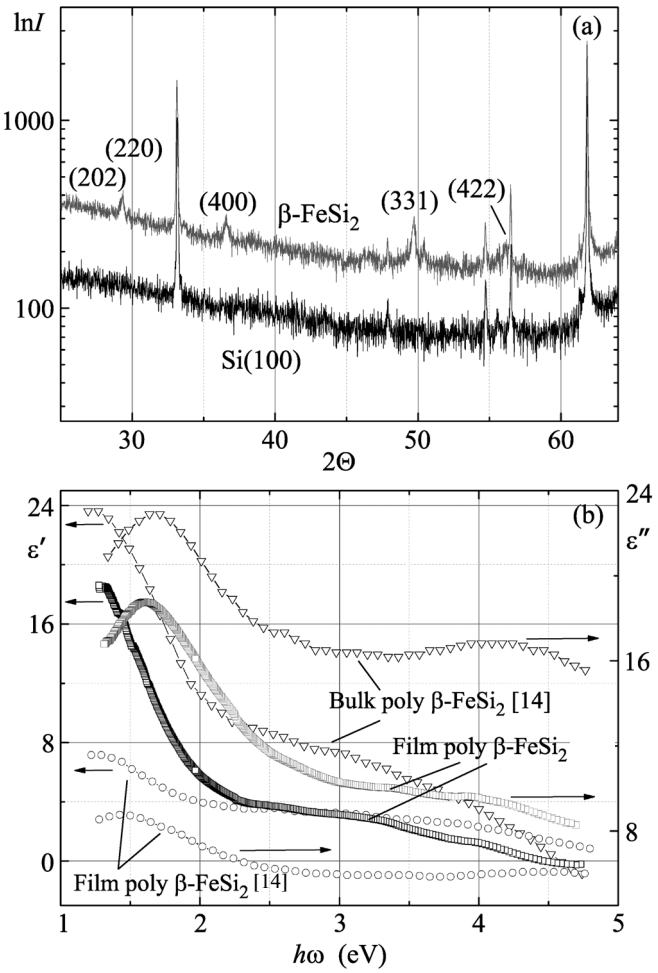

Fig. 2. (a) X-ray diffraction pattern for the β-$FeSi_2$/Si(100) film and pure Si(100) substrate. (b) Energy dependence of the real and imaginary parts of the relative permittivity for the 40-nm-thick polycrystalline β-$FeSi_2$/Si(100) film.

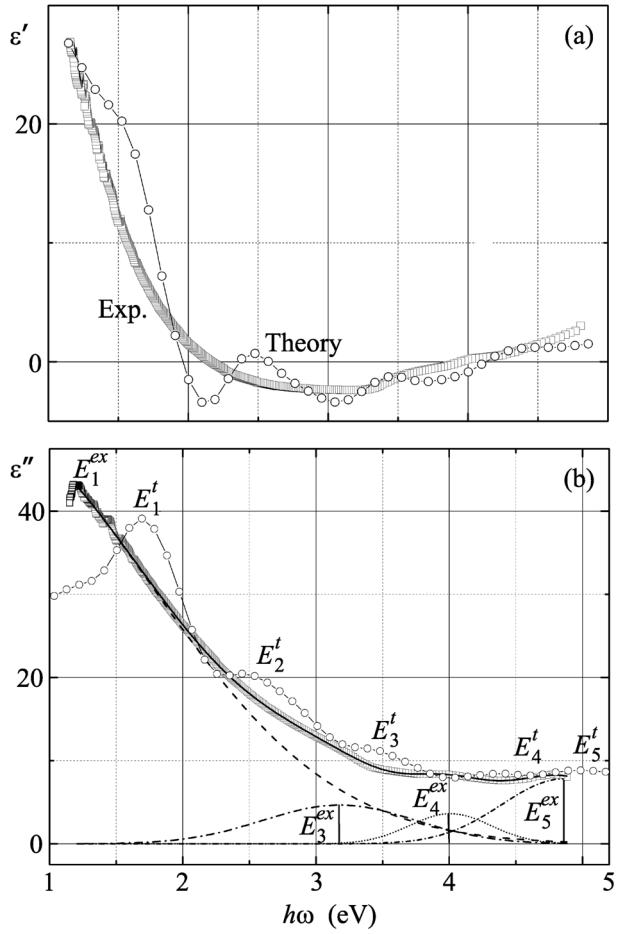

Fig. 3. Energy dependence of the (a) real and (b) imaginary parts of the relative permittivity for the 27-nm-thick epitaxial Fe_3Si film. Experimental data at $T = 296$ K (squares) are compared to the results of calculations for $T = 0$ (circles). The solid line is the fit by the sum of Gaussian components (E_1–E_4).

width of each of these peaks ΔE exceeds 1 eV. Comparing their positions on the energy axis ($E_1^{ex}-E_1^t$, $E_3^{ex}-E_3^t$, $E_4^{ex}-E_4^t$, and $E_5^{ex}-E_5^t$), we can determine the shifts of the positions of the absorption bands. Energies E_1^{ex}, E_3^{ex}, and E_4^{ex} are shifted by about 0.5 eV, whereas E_5^{ex} is shifted by 0.26 eV, which is less than the peak width ΔE. The E_3^t band is indistinguishable on the experimental ε" curve. The shift and smearing of the bands can be caused by a whole set of different mechanisms and phenomena in the prepared Fe_3Si film. Among them, there can be dislocations and stacking faults arising in the course of the island coalescence as well as the disorder in the positions of Si and Fe atoms. Indeed, according to [23, 24], silicon atoms are able to substitute iron atoms. In addition, a certain contribution can come from the thermal processes. Another possible cause of the quantitative difference between the calculations and the experimental data can stem from the underestimation of the electron correlation effects in the GGA. At the same time, our experimental data disagree with the results of calculations of the real and imaginary parts of the relative permittivity reported in [9].

The spectrum of the imaginary part of relative permittivity is formed owing to the interband electron transitions from the occupied states to the empty ones. As a rule, the absorption bands are rather broad and overlap each other. Analyzing the VASP calculations of the partial density of states for spin-polarized charge carriers in Fe_3Si iron silicide (Fig. 4), we reveal the most probable interband transitions. Their energies are listed in the table. The contribution introduced by the electronic shell of silicon atoms to the

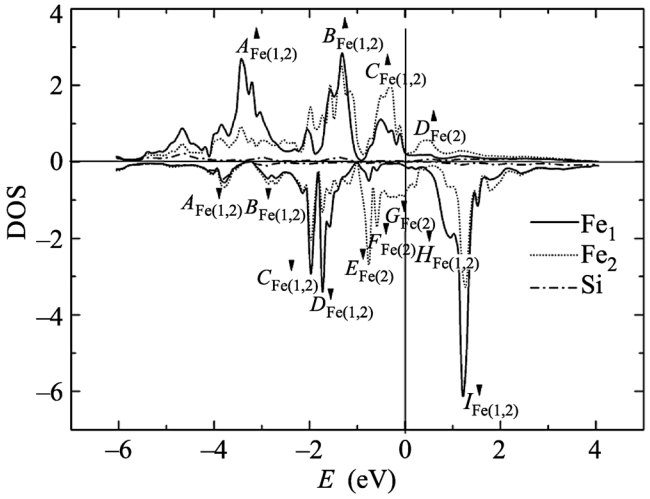

Fig. 4. Partial densities of states (PDOS) for the spin-polarized charge carriers in bulk Fe_3Si iron silicide. The arrows denote spin directions.

formation of the absorption spectrum is very small (see Fig. 4); therefore, we neglected the transitions related to silicon.

The data represented in the table allow giving a qualitative interpretation of the mechanisms underlying the nature of peaks in the absorption spectrum. We see that the calculated values of the peak positions are systematically shifted by about 0.5 eV with respect to those determined in experiment.

5. Summarizing, we can say that, in the present work, we have experimentally determined the energy dependence of the relative permittivity ε of a 27-nm-thick epitaxial Fe_3Si iron silicide film on a Si(111) single-crystalline silicon substrate within the energy range $E = 1.16$–4.96 eV. The experimentally determined dispersion law of ε is in qualitative agreement with that calculated in the framework of the density functional theory. The calculated ε'' spectrum is shifted toward higher energies with respect to that determined in experiment. This probably results from the structural imperfection of the film, whereas the calculations are based on the assumption of perfect crystal structure. We demonstrate that formation of a continuous layer of Fe_3Si iron silicide film occurs when the film thickness exceeds 5 nm.

Positions of the optical absorption peaks and calculated possible interband transitions (in electronvolts)

Peak	Peak energy (experiment)	Peak energy (theory)	Most probable interband transitions
E_1	1.2	1.7	$E_{Fe(2)}\downarrow\rightarrow I_{Fe(1,2)}\downarrow$ (1.96); $E_{Fe(2)}\downarrow\rightarrow H_{Fe(1,2)}\downarrow$ (1.71); $B_{Fe(1,2)}\uparrow\rightarrow D_{Fe(2)}\uparrow$ (1.71)
E_2	–	2.66	$D_{Fe(1,2)}\downarrow\rightarrow I_{Fe(1,2)}\downarrow$ (2.93); $D_{Fe(1,2)}\downarrow\rightarrow H_{Fe(1,2)}\downarrow$ (2.68)
E_3	3.16	3.62	$B_{Fe(1,2)}\downarrow\rightarrow I_{Fe(1,2)}\downarrow$ (3.99); $B_{Fe(1,2)}\downarrow\rightarrow H_{Fe(1,2)}\downarrow$ (3.74)
E_4	4	4.49	$A_{Fe(1,2)}\downarrow\rightarrow H_{Fe(1,2)}\downarrow$ (4.6); $A_{Fe(1,2)}\uparrow\rightarrow D_{Fe(2)}\uparrow$ (4)
E_5	4.84	5.13	$A_{Fe(1,2)}\downarrow\rightarrow I_{Fe(1,2)}\downarrow$ (4.96)

This work was supported by the Russian Foundation for Basic Research (project nos. 13-02-01265 and 14-02-31309), by the Council of the President of the Russian Federation for Support of Young Scientists and Leading Scientific Schools (project no. NSh-2886.2014.2), by the Russian Ministry of Education and Science (state contract no. 02.G25.31.0043), and by the Presidium of the Russian Academy of Sciences (program no. 24.34).

REFERENCES

1. H. Haiji, K. Okada, T. Hiratani, M. Abe, and M. Ninomiya, J. Magn. Magn. Mater. **160**, 109 (1996).
2. M. Hong, H. S. Chen, J. Kwo, A. R. Kortan, J. P. Mannaerts, B. E. Weir, and L. C. Feldman, J. Cryst. Growth **111**, 984 (1991).
3. Y. Maeda, T. Ikeda, T. Ichikawa, T. Nakajima, B. Matsukura, T. Sadoh, and M. Miyao, Phys. Proc. **11**, 200 (2011).
4. K. Hamaya, K. Ueda, Y. Kishi, Y. Ando, T. Sadoh, and M. Miyao, Appl. Phys. Lett. **93**, 132117 (2008).
5. H. Y. Hung, S. Y. Huang, P. Chang, W. C. Lin, Y. C. Liu, S. F. Lee, M. Hong, and J. Kwo, J. Cryst. Growth **323**, 372 (2011).
6. T. Yoshitake, D. Nakagauchi, T. Ogawa, M. Itakura, N. Kuwano, and Y. Tomokiyo, Appl. Phys. Lett. **86**, 262505 (2005).
7. Y. Ando, K. Hamaya, K. Kasahara, K. Ueda, Y. Nozaki, T. Sadoh, Y. Maeda, K. Matsuyama, and M. Miyao, Appl. Phys. Lett. **94**, 182105 (2009).
8. Y. Fujita, S. Yamada, Y. Ando, K. Sawano, H. Itoh, M. Miyao, and K. Hamaya, J. Appl. Phys. **113**, 013916 (2013).
9. S. Naderizadeh, S. M. Elahi, M. R. Abolhassani, F. Kanjouri, N. Rahimi, and J. Jalilian, Eur. Phys. J. B **85**, 144 (2012).
10. I. A. Tarasov, N. N. Kosyrev, S. N. Varnakov, C. G. Ovchinnikov, S. M. Zharkov, V. A. Shvets, S. G. Bondarenko, and O. E. Tereshchenko, Tech. Phys. **57**, 1225 (2012).
11. I. A. Yakovlev, S. N. Varnakov, B. A. Belyaev, S. M. Zharkov, M. S. Molokeev, I. A. Tarasov, and S. G. Ovchinnikov, JETP Lett. **99**, 527 (2014).
12. D. Barton and F. K. Urban III, Thin Solid Films **516**, 119 (2007).
13. F. K. Urban III, D. Barton, and T. Tiwald, Thin Solid Films **518**, 1411 (2009).

14. C. A. Dimitriadis, J. H. Werner, S. Logothetidis, M. Stutzmann, J. Weber, and R. Nesper, J. Appl. Phys. **68**, 1726 (1990).
15. G. Kresse and J. Hafner, Phys. Rev. B **47**, 558 (1993).
16. G. Kresse and J. Hafner, Phys. Rev. B **49**, 14251 (1994).
17. G. Kresse and J. Furthmüller, Phys. Rev. B **54**, 11169 (1996).
18. P. E. Blochl, Phys. Rev. B **50**, 17953 (1994).
19. G. Kresse and G. D. Joubert, Phys. Rev. B **59**, 1758 (1999).
20. J. P. Perdew, K. Burke, and M. Ernzerhof, Phys. Rev. Lett. **77**, 3865 (1996).
21. H. J. Monkhorst and J. D. Pack, Phys. Rev. B **13**, 5188 (1976).
22. M. Gajdos, K. Hummer, G. Kresse, J. Furthmüller, and F. Bechstedt, Phys. Rev. B **73**, 045112 (2006).
23. L. Dobrzynski, J. Phys.: Condens. Matter **7**, 1373 (1995).
24. G. A. Al-Nawashi, S. H. Mahmood, A. D. Lehlooh, and A. S. Saleh, Physica B **321**, 167 (2002).

Translated by K. Kugel